Spacer flashover in Gas Insulated Switchgear (GIS) with humid SF6 under different electrical stresses

Purnomoadi, A.P.; Mor, A. Rodrigo; Smit, J.J.

DOI
10.1016/j.ijepes.2019.105559

Publication date
2019

Document Version
Final published version

Published in
International Journal of Electrical Power & Energy Systems

Electrical Power and Energy Systems 116 (2020) 105559

Contents lists available at ScienceDirect

Electrical Power and Energy Systems

journal homepage: www.elsevier.com/locate/ijepes

Spacer flashover in Gas Insulated Switchgear (GIS) with humid SF_6 under different electrical stresses

A.P. Purnomoadi[a], A. Rodrigo Mor[b], J.J. Smit[b]

[a] Transmission and Distribution R&D, PLN Research Institute, Jakarta, Indonesia
[b] Electrical Sustainable Energy, Delft University of Technology, Delft, the Netherlands

ARTICLE INFO

Keywords:
Gas insulated switchgear
Gas insulated substation
GIS
Tropical conditions
Humid insulating gas
Spacer flashover
SF_6

ABSTRACT

Humid insulating gas (SF_6) has been observed in a case study of 631 CB-bays of Gas Insulated Switchgear (GIS) operating under tropical conditions. The routine gas quality check in the case study reported that 20% of the non-Circuit Breaker enclosures have humidity above the value recommended by the IEEE and IEC standards. Therefore, an investigation into the flashover characteristics of a spacer in humid SF_6 has been initiated in the High Voltage Laboratory of TU Delft, The Netherlands. The setup is a small model resembling the insulation system of a GIS with controlled parameters of humidity content and gas pressure. The electrical stresses in the test are AC, LI+, LI−, and SI with homogeneous, quasi-homogeneous-, and inhomogeneous field configurations. In general, the humidity does not influence the withstand strength of the spacer as long as there is no condensation. When condensation occurred, the flashover voltage dropped by 28% during the test under AC at 2.6 bars, and by 38% during the test under LI+ at 2.5 bars; both with quasi-homogeneous field configuration. In the test with homogeneous field setup, the flashover voltage was dropped by 67% under LI+ at 3.4 bars. In our setup, it has also been observed that the flashover-drop due to condensation is higher than due to a 2-mm aluminum particle attached to the sample close to the high electric field region simulating the inhomogeneous field configuration.

1. Introduction

Gas Insulated Switchgear (GIS) has been known to be reliable for more than 40 years. One of the reasons is because the active components are installed inside sealed-enclosures that reduce the environmental stress. However, in our case study failure rates over twice the value reported by the 3rd CIGRE survey of 2007 have been observed [1]. The case study consists of 631 CB-bays of 500 kV and 150 kV GIS which are located in 79 locations in Java and Bali, two main tropical islands of Indonesia.

Former investigations [2] reported that 66% of the failures were due to the breakdown of the primary dielectric subsystem, where the tropical parameters might be involved indirectly. Some possible failure modes are as follows:

- Humid environment accelerates corrosion at the exposed parts of GISs, especially for outdoor installations. Corrosion on enclosure-joints contributes to the gas-leaking, which is dominantly found in the case study.
- The warm temperature causes constant desorption of moisture, mostly from the spacer, that creates humidity in the insulating gas in GIS compartments. The routine gas quality check reported that 20% of the non-Circuit Breaker enclosures have humidity above the value recommended by IEEE and IEC standards [3,4]. Humid gas in combination with Partial Discharge (PD) produces by-products that reduce the withstand strength, particularly the solid by products [2].
- The frequent lightning incidence increases the electrical transient stress on the insulation system, particularly, when the surge arrester fails.

In GIS, there are two regions of the insulation system to be considered separately: (1) the SF_6 gas including its interface to the solid insulating or conducting materials, and (2) the internal bulk of the solid insulating material. All dielectric failures found in the case study were located in the first region [2].

A laboratory setup has been constructed in the High Voltage Laboratory in TU Delft, the Netherlands, to find the influence of humidity on the flashover of a spacer. The model consists of a cast epoxy-resin sample and SF_6 resembling the insulation system of a GIS. The controlled parameters in the tests are the humidity-content and the gas pressure, while the temperature is kept constant at 20 °C, which represents the possible lowest temperature in the tropics. The gas pressure has been adjusted to represent the real operating condition. The

E-mail addresses: a.p.purnomoadi@tudelft.nl (A.P. Purnomoadi), A.RodrigoMor@tudelft.nl (A. Rodrigo Mor), J.J.Smit@tudelft.nl (J.J. Smit).

https://doi.org/10.1016/j.ijepes.2019.105559
Received 19 February 2019; Received in revised form 24 June 2019; Accepted 17 September 2019

electrical stresses under investigation are AC, Lightning Impulse (LI) + and −, and Switching Impulse (SI). The setup makes possible three configurations of electric field distributions, namely a homogeneous configuration, a quasi-homogeneous configuration, and a configuration with a particle attached on the spacer to simulate an extreme inhomogeneous field in GIS.

2. Origin of moisture in GIS

The terms moisture and humidity have a different meaning. Moisture refers to the water molecules bonded on the surface (adsorbed-moisture) or in the structure of solids (absorbed-moisture) [3]. Meanwhile, humidity refers to the water molecules in vapor form within a background gas [3]. It is worth to mention that the regular gas quality check measures the humidity, not the moisture.

The moisture infiltrates into the GIS by at least two mechanisms [3,5]. The first is through the leaking points on the enclosure, and the second is due to the desorption of moisture from the spacer, the conductor and the internal surface of the enclosure. The previous observations [2] concluded that most of the moisture comes by the second mechanism. The following paragraphs summarize the report.

To investigate the amount of humidity inside different enclosures in GIS more than 3000 data of humidity-content have been collected in the case study. The Cumulative Distribution Functions (CDF) for humidities measured in the Circuit Breaker (CB) and Non-CB Enclosures of 150 kV GISs are given in Fig. 1. Every point in the graph represents the value of humidity (in ppmV), in GIS enclosures with a service time of more than ten years. The data were taken during the afternoon with gas temperatures within 30–33 °C. The enclosures have been grouped based on the type of active components (i.e., CB or non-CB enclosure), and the manufacturer.

Fig. 1 gives the following interpretations:

- The amount of humidity is characteristic for the different manufacturers and the kind of the active component inside the GIS enclosure. For example, the red-line in Fig. 1.b shows that a small fraction of humidity content in the non-CB enclosures of GIS from the manufacturer A has a value above 1000 ppmV. The high values come from the termination, where the layers of insulating tapes contain much of the absorbed moisture. The same figure also shows a black-line with an enormous amount of humidity in GIS from the manufacturer D which doesn't use desiccants.
- By comparing the lines in Fig. 1.a and b from the same manufacturer, it can be seen that the humidity content in the CB is lower than in the non-CB enclosure. The reason is that the SF_6 density and the number of desiccants is higher in comparison to the non-CB enclosure. All humidity content from all manufacturers is below the limit from the IEEE and IEC. Only a small fraction for make A is beyond its manufacturer's limit.

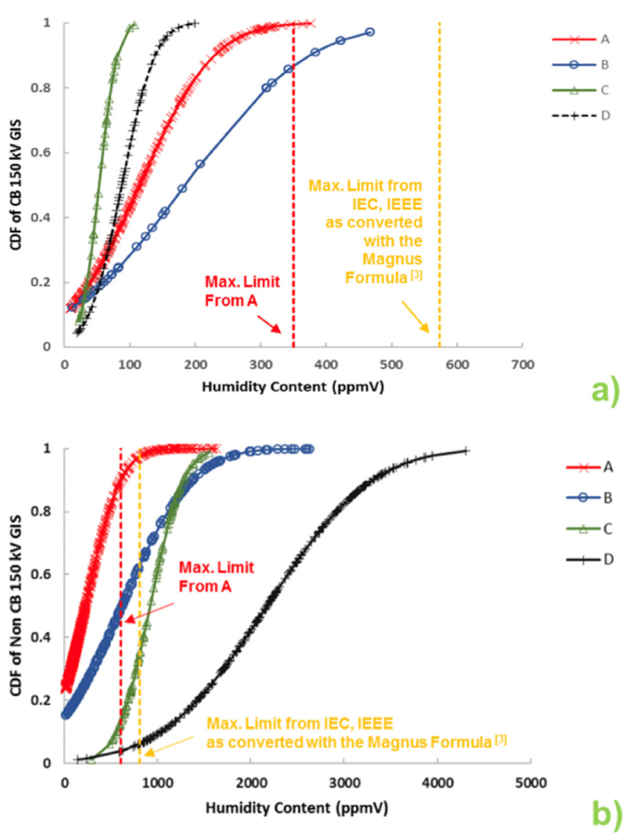

Fig. 1. The CDF of humidity in CB (a) and Non-CB (b) enclosures from 4 different manufacturers (A, B, C, D) of 150 kV GIS in the case study. The maximum limit of humidity content from the manufacturer A and the IEEE [3] and IEC [4] are also given in the graph assuming the gas pressure in CB and non-CB compartments, sequentially 7 bars and 5 bars.

The other observation has been conducted on the humidity content of 20 enclosures with leaking points. The leakage rate is recorded regularly as well as the amount of SF_6 for topping up, before any repair action. By comparing the humidity content in the leaking enclosure with another sound and identical enclosure (with the same shape, current loading, and ambient conditions), there was no correlation between the humidity content and whether there is a leak on the enclosure. The latter finding leads to the interpretation that the amount of moisture passing through a leaking point is considerably neglectable. In all probability most of the moisture in GIS originates from the "absorbed" moisture in solid insulation and the "adsorbed" moisture at the metallic surface like in conductors or enclosures [3,6].

In conclusion, the amount of moisture in GIS depends on the following factors, 1. GIS design (like the volume of desiccants, density of SF_6, type of material, dimension of enclosure and spacer), 2. GIS handling (including how to keep the parts dry during transportation, erection, and maintenance; duration of vacuuming after erection or after maintenance with opening the enclosure).

3. Spacer with humid SF_6 in GIS

In humid insulating gas, a high amount of water molecules (H_2O) dilutes into the gas system (see the illustration in Fig. 2). The presence of water molecules influences the withstand voltage of the insulating gas by two opposite mechanisms, i.e., the presence of humidity will reduce the withstand strength by lowering the density of the gas system [5], and on the other hand, since water is also an electronegative gas

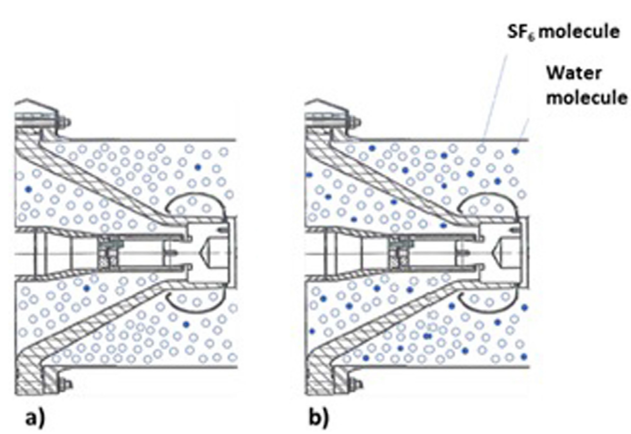

Fig. 2. Illustration between dry (figure a) and humid (figure b) insulating gas in GIS.

[7], the presence of a water molecules can improve the withstand strength of the gas system.

However, the interest of the current research is on the influence of humid SF_6 to the withstand of the gas-solid interface. The presence of humidity (i.e., the moisture in the form of gas) hypothetically will not influence on the breakdown of the gas-solid interface, as long it does not perturb the surface condition of the solid insulation. However, in particular condition, the moisture may turn into water or ice. The water has a dielectric constant of 80, while ice is 2. The presence of water droplets on the insulator surface will raise electric field in many locations of the solid insulation surface that decrease the withstand strength.

Laboratory tests have been carried out to investigate which mechanism is more dominant than the other.

4. Experiment setup

The setup mainly consists of three parts, i.e., a chamber with the sample and the electrodes, a vessel for mixing the SF_6 with humidity, and a setup for voltage generation. The next subsections give the details.

4.1. Electrode configurations in the test chamber

The test chamber is a miniature of "spacer-and-gas" model. A cylindrical epoxy resin sample (representing a spacer) is placed in between two electrodes made of stainless steel inside a small chamber and is filled with an SF_6 and H_2O mixture (see Fig. 3). The volume of the gas in the vessel is 60 ml.

Two electrode configurations were used to simulate three electric field distributions on the surface of the epoxy sample, namely:

1. *Homogeneous field configuration*, where the electric field parallel to the sample's cylindrical surface is constant at any location.
2. *Quasi-homogeneous field configuration*, where the electric field parallel to the sample has a declining slope from the maximum to the minimum (which is representing the coaxial configuration of GIS).
3. *Inhomogeneous field configuration*, where a particle is attached on the epoxy close to the electrode so that a very high electric field appears at both tips of the particle.

The field-factor has been introduced to measure the degree of homogeneity of the electric field distribution on the sample [8]. The field-factor (F) is the ratio between the maximum and the average electric field along the surface of the sample. The homogeneous configuration, ideally, has a field factor of 1 (in the test F = 1.2), the quasi-homogeneous configuration has a field factor between 1 and 5 (in the test F = 1.9), while the inhomogeneous configuration has a field factor beyond 5 (in the test, the F depends on the shape of the tips at the attached particle) [8].

During the design for the test, this factor was estimated by a simulation in COMSOL®. Fig. 4 gives a simulation result with quasi-homogeneous configuration along with the electric field distribution of real spacer.

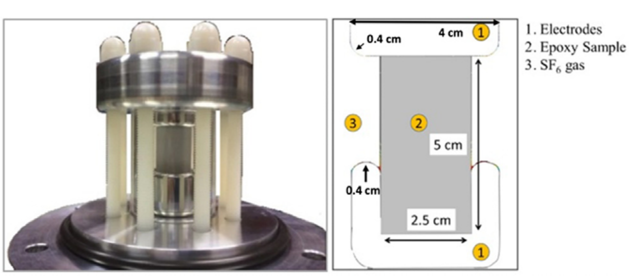

Fig. 3. The test-vessel with an epoxy sample placed in the middle of the quasi-homogeneous configuration. The right picture shows the schematic diagram.

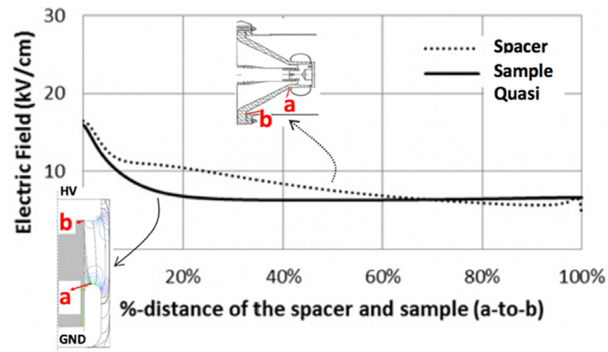

Fig. 4. A normalized electric field distribution (from a to b) on a 420 kV conic spacer and on the epoxy sample with a quasi-homogeneous configuration.

4.2. Material specification and dimension of the sample

A GIS spacer is usually made of epoxy resin with different kinds of fillers such as alumina and silica. Spacers of alumina fillers are known to have better withstand against the surface tracking [9]. The laboratory test used epoxy with silica fillers with a purpose to observe the flashover traces and to be representative with existing GIS materials. All samples have a cylindrical shape with a diameter of 25 mm. Table 1 gives the specification of the epoxy.

4.3. Gas pressures in the test

From the observation in the case study, humid insulating gas was mostly found in the non-CB enclosures with single-phase enclosure configuration. Therefore, the gas pressures in the test have been adjusted to represent such condition. Table 2 gives operating gas pressures of GIS from 4 major manufacturers in the case study. In this document, except mentioned differently, all values of gas pressures are in bar-absolute.

As seen in Table 2, the non-CB enclosures in GIS with a single-phase configuration have pressures between 3.3 and 5.3 bars (at 20 °C). Therefore, the investigated gas pressures were within 1 up to 6 bars. However, the value was also limited by the capability of the setup, for example, the test with AC was only up to 3 bars due to the capacity limit of the power transformer.

4.4. Humidity manipulation in the test chamber

Four kinds of humidity levels have been simulated in the tests, namely (the humidity content is within the brackets), dry (100–1000 ppmV), humid (2000–6000 ppmV), saturated, and condensation. The "dry" condition is defined when no humidity has been added into the SF_6 gas. Two sources of dry SF_6 gas were used during the test, with maximum humidity content of 1000 ppmV. The gas manipulation was done inside a "mixing vessel" as seen in Fig. 5. The procedure was as follows:

Table 1
Material specification of the epoxy sample used in the tests.

Specification			
Resin Type	Solid epoxy resin based on bisphenol A		
Hardener	Phthalic anhydride PSA		
Filler	Quartz LM-10		
Parameter	**Unit**	**Value**	**Measurement Standard**
Loss Factor (Tan δ)	%	2.2	IEC 60250, 50 Hz, 20 °C
Dielectric Constant (ε_r)	–	4.1	IEC 60250, 50 Hz, 20 °C

Table 2
Operating gas pressures in GIS in the case study.

Manf.	Phase Conf.	Rated kV	CB	Other than CB
			Operational Pressure ($\mathbf{bar_a}$, 20°C)	Operational Pressure ($\mathbf{bar_a}$, 20°C)
A	1-ph	525	7.5	5.3
	1-ph	170	7	3.3
	3-ph	170	7.9	7.1
B	3-ph	170	9.6	9.6
C	1-ph	170	7.2	4.8
D	3-ph	170	5.9	5.9

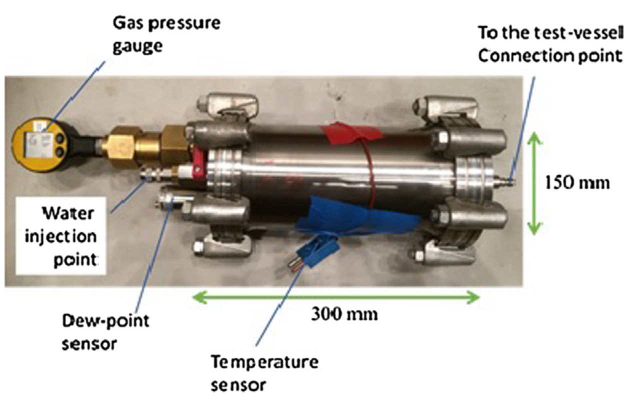

Fig. 5. The mixing vessel where the SF_6 and the water vapor were mixed.

4.4.1. The creation of humid gas

The air inside the mixing vessel was firstly evacuated to 0.2 mbar. Afterwards, a prescribed amount of demineralized water (with a volume of 0.05–0.2 ml) was injected into the mixing vessel. At 0.2 mbar, the water evaporates at 20 °C. Following this step, the SF_6 was slowly injected into the mixing vessel up to the investigated gas pressure. The amount of humidity was monitored by the built-in dew point sensor inside the mixing-vessel. The conversion from dew point (T_d, in °C) into ppmV was based on the Magnus Formula [10]. After 15–30 min of stabilization time, the humid SF_6 was slowly transferred into the test chamber (which was formerly also evacuated to 0.2 mbar) through a connection point.

4.4.2. The creation of saturating gas

The procedure was similar as in humid gas, but the prescribed water injected into the mixing vessel was within 0.5–1 ml. The saturation was indicated when the dew-point temperature, T_d, equals the room temperature (T_a).

4.4.3. The creation of condensation

Firstly, the air inside the mixing vessel and test chamber was evacuated down to 0.2 mbar. Afterwards, a high amount of demineralized water (1–3 ml of volume) was injected into both chambers. This step was to ensure both chambers have a very humid condition inside of them. The next step was slowly letting the SF_6 coming into the mixing-vessel up to the investigated pressure. After stabilization time, the humid gas was transferred into the test chamber.

4.5. Voltage Generation

The voltage generation setups are presented in Fig. 7 (for AC) and Fig. 8 (for LI and SI). During the test, the test chamber was mounted into a GIS setup as seen in Fig. 6. Once a breakdown observed, a

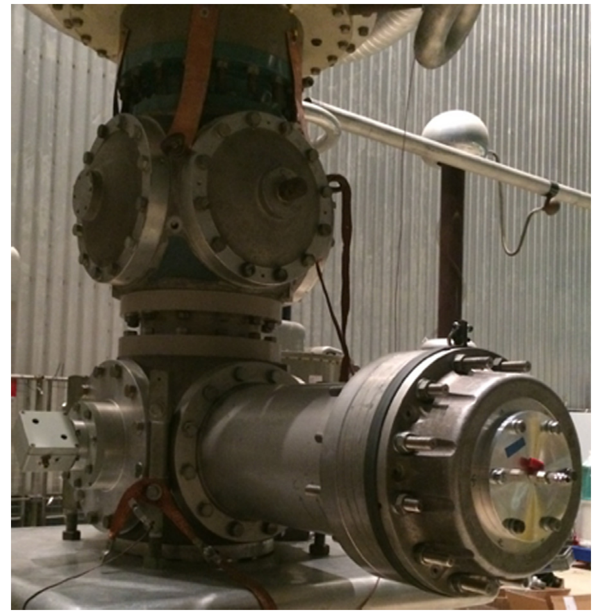

Fig. 6. GIS setup for voltage application. During the test, the test chamber was installed inside the setup.

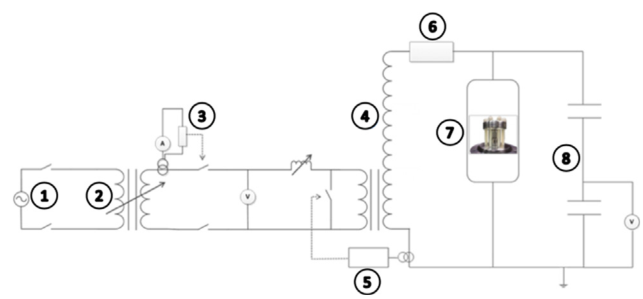

Fig. 7. AC Voltage Generation Setup. 1. 220 V-AC grid; 2. Voltage regulator; 3. Current limiter; 4. Power transformer; 5. High-speed tripping circuit; 6. Damping resistor; 7. Test chamber; 8. Capacitive voltage divider.

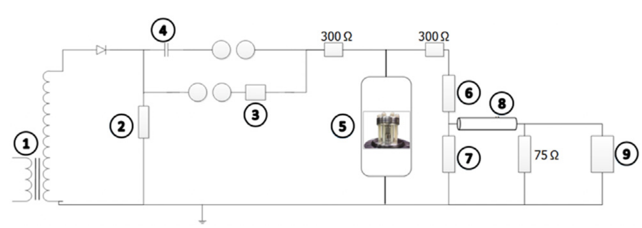

Fig. 8. Setup for Impulse Generation. 1. Power transformer; 2. Front resistance; 3. Tail resistance; 4. A discharging capacitance; 5. Test object; 6. Voltage divider-high resistive part; 7. Voltage divider-low resistive part; 8. Coaxial cable; 9. Digital Monitoring System (DMS).

relaxation time of 10–15 min was taken before the next voltage application.

4.5.1. AC voltage generation

A single-phase power transformer provided the AC voltage with a maximum capacity of 200 kVA. The high voltage side of the power transformer was connected to the GIS, while an auxiliary winding was attached at the low voltage side to regulate the voltage output. A high-speed tripping circuit was installed to limit the flashover current that allows several breakdowns on one sample. The voltage raised from zero in steps of 20 kV and 1 kV/second rate.

Table 3
Summary of laboratory tests. The column gives the electrode configuration, while the row gives the voltage stress.

Voltage Stress		Electrode Configuration: Homogeneous – Humidity (ppmV)	Homogeneous – Gas Pressure (bar$_a$)	Quasi-homogeneous – Humidity (ppmV)	Quasi-homogeneous – Gas Pressure (bar$_a$)	Inhomogeneous (w/ particle attached on spacer) – Humidity (ppmV)	Inhomogeneous (w/ particle attached on spacer) – Gas Pressure (bar$_a$)
	AC	None		1000	1-3	None	
				2000	1-3		
				4000	1-3		
				6000	1-3		
				Sat.	1-3		
				Cond.	2 and 2.5		
	LI+	100	2-3	1000	1-4	100	3.5 and 4.3
		2000	2-3.5	4000	1-4	3000	3.5 and 4
		Cond.	3.5 & 4.5	6000	1-4	6000	3.2 and 3.8
				Sat.	1-3		
				Cond.	2 and 2.5		
	LI-	None		1000	1-4	100	3.5 and 4.4
				Sat.	1-4		
	SI	100	2.5-6	1000	2.5-6	None	
		2000	2.5-5.2	3000	2.5-6		
		4000	3.5-4.5	4000	2.5-6		
		Sat.	3.2-5	6000	2.5-5		

*Sat.= saturation, Cond.= condensation

4.5.2. LI and SI voltage generation

Ten stages of the Marx Generator in the HV Laboratory in TU Delft had been used to generate the Lightning Impulse (+/−) and the Switching Impulse with shapes following the IEC 60060-1:2010 standard [11]. Each impulse started from about 50% of the estimated breakdown voltage, and then increased in 20 kV steps.

5. Experimental results

Most of the tests were done with the quasi-homogenous field configuration. Table 3 gives the summary of the tests in a matrix with the voltage stress and the electrode configuration. The test with homogeneous setup was only under LI+ and SI, while tests with a particle-attached on the spacer were done under LI+ and LI−.

The following subsections, A to C, will present the graphs. The humidity content is stated by the last number of the legend in each graph. A minimum number of 3 flashovers were recorded for every point in the graphs.

5.1. Flashover voltage in quasihomogeneous configuration

The test with the quasi-homogeneous configuration has been conducted under AC, LI+, LI−, and SI stresses. The test with saturated gas was simulated only under AC, LI+, and LI−; while the test with condensation was done only under AC and LI+. The investigated gas pressures are as follow:

1. Under AC Voltage: 1–3 bars.
2. Under LI+/−: 1–4 bars.
3. Under SI: 2–6 bars.

The flashover voltage under AC was recorded in kV-peak/√2, while the results from LI and SI were in kV-peak. Fig. 9 presents the flashover voltage from the test with the quasi-homogeneous setup with all kinds of voltage stress. Meanwhile, Figs. 10–12 sequentially give the flashover of the same setup under AC, LI, and SI.

According to Fig. 9, in general, the flashover under LI is higher than the value under SI and AC. A standard deviation above 10% has been

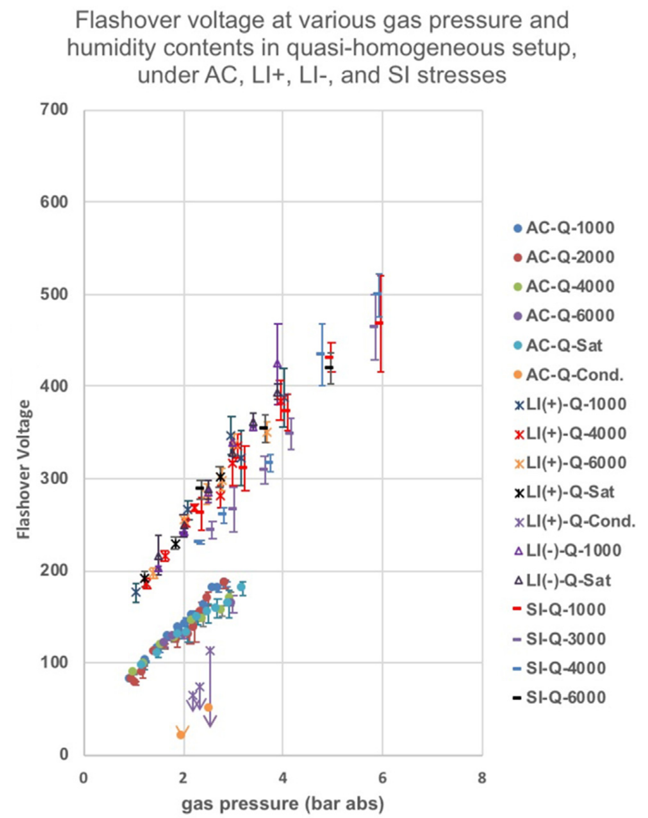

Fig. 9. The flashover voltage as a function of gas pressure at various humidity contents in the quasi-homogeneous setup under AC, LI +/− and SI Voltage Stresses. For AC, the value is in kV-peak/√2, while LI and SI are in kV-peak. The arrow pointing down means that the subsequent flashover voltage is consistently decreasing.

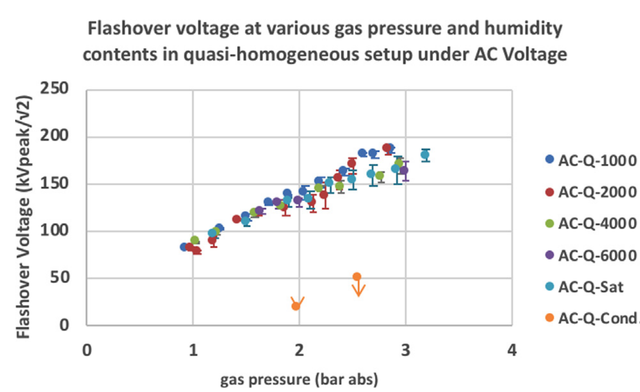

Fig. 10. The flashover voltage as a function of gas pressure at various humidity contents in the quasi-homogeneous setup under AC voltage stress. The value is in kV-peak/√2. The arrow pointing down means that the subsequent flashover voltage is consistently decreasing.

observed in the flashover values from all voltage stresses, especially at the higher gas pressures. The later is probably because the surface deterioration on electrodes are more varying at the higher flashover voltages.

Figs. 10–12 show that the flashover voltage is increasing as a function of gas pressure. This tendency agrees that at the higher pressure, the insulating gas density, mainly the SF_6, becomes higher. On the other hand, the variation of humidity content does not influence to the flashover voltage, except when condensation occurs as shown in Fig. 10 (in the test with AC) and 11 (in the test with LI+).

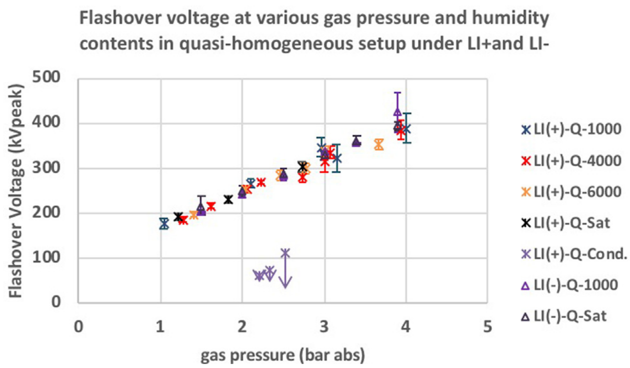

Fig. 11. The flashover voltage as a function of gas pressure at various humidity contents in the quasi-homogeneous setup under LI+ and LI− voltage stresses. The value is in kV-peak. The arrow pointing down means that the subsequent flashover voltage is consistently decreasing.

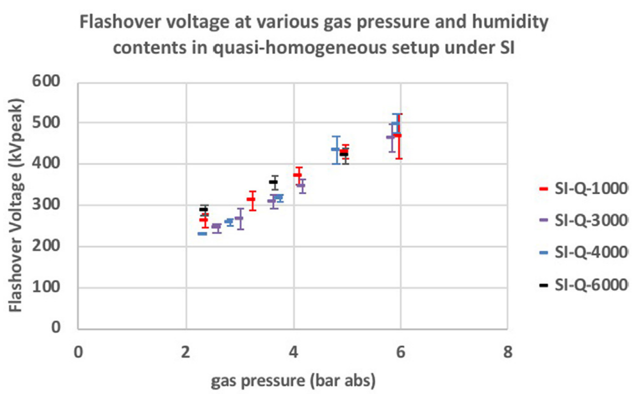

Fig. 12. The flashover voltage as a function of gas pressure at various humidity contents in the quasi-homogeneous setup under SI. The value is in kV-peak.

5.2. Flashover voltage in homogeneous configuration

The test with the homogeneous configuration has been conducted under LI+ and SI voltage stresses. The saturating-gas has been tested under SI, while the condensation has been tested under LI+. The gas pressures are as follow:

1. Under LI+: 2–4.5 bars.
2. Under SI: 2–6 bars.

The flashover voltage was recorded in kV-peak. Fig. 13 presents the flashover voltage from the test with the homogeneous setup with LI+ and SI, while details are provided in Figs. 14 and 15.

By comparing the results in Figs. 9 and 13, in general, the flashover voltage is higher in the test with a homogeneous setup rather than in the quasi-homogeneous setup at a similar gas pressure and humidity content. This finding is in line with our expectations since a breakdown is a function of the electric field, and a higher voltage is needed in the homogeneous configuration to develop a similar electric field as in non-homogeneous configuration.

Figs. 14 and 15 show the similar tendency as in the test with quasi-homogeneous setup, where the humidity content does not influence the flashover voltage, as long there is no condensation.

5.3. Flashover voltage in the setup with a particle attached on the sample

Fig. 16 shows the setup where a 2-mm aluminum particle with a radius of 0.25 mm was attached on the epoxy sample close to the maximum curvature of the electrode where a high electric field occurs.

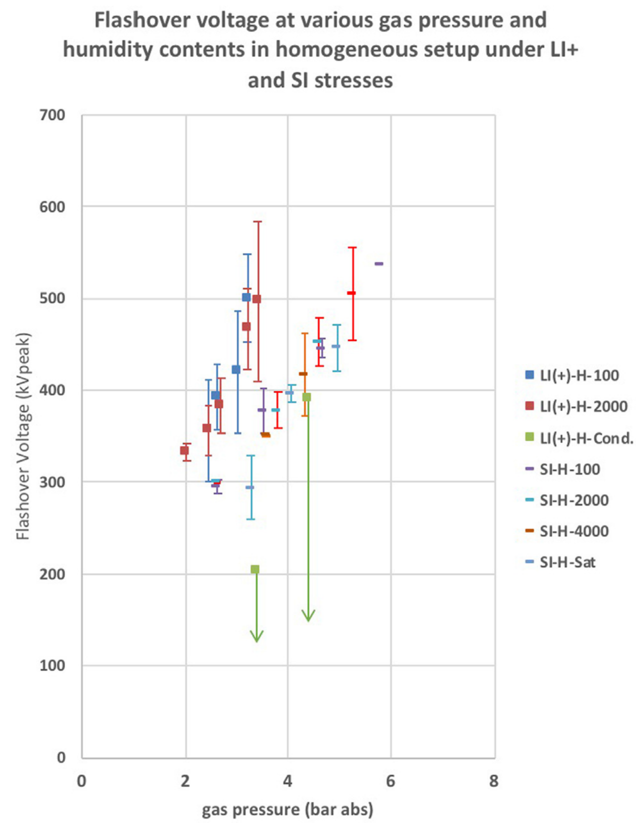

Fig. 13. The flashover voltage as a function of gas pressure at various humidity contents in the homogeneous setup under LI+ and SI voltage stresses. The value is in kV-peak. The arrow pointing down means that the subsequent flashover voltage is consistently decreasing.

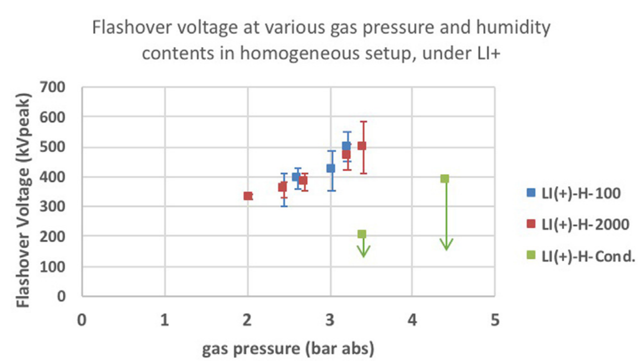

Fig. 14. The flashover voltage as a function of gas pressure at various humidity contents in the homogeneous setup under LI+ voltage stresses. The value is in kV-peak. The arrow pointing down means that the subsequent flashover voltage is consistently decreasing.

The test has been conducted under LI+ (with a humidity content of 100, 3000, and 6000 ppmV) and LI− (with a humidity content of 100 ppmV) representing the highest electrical stress in operating condition. The procedure of the test was more difficult than the previous tests because only one breakdown was allowed on one sample. Two samples were used per test on single gas pressure.

The investigated gas pressures were limited to only two points within 3 and 4.5 bars. Fig. 17 gives the result.

As seen in the figure above, the flashover voltage is proportionally increasing with the gas pressure, except in the test with a humidity content of 6000 ppmV under LI+.

From the test with LI+, the flashover tends to decrease as the humidity content is increasing from 100 to 3000 ppmV. However, the

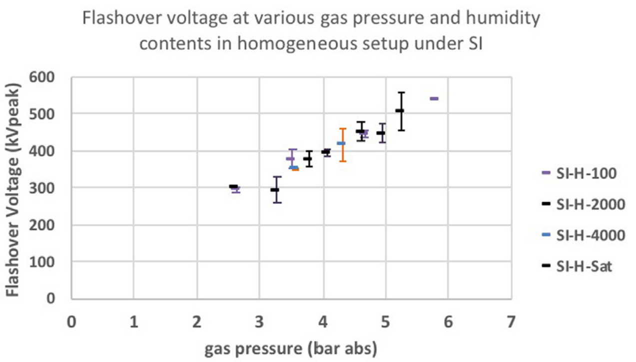

Fig. 15. The flashover voltage as a function of gas pressure at various humidity contents in the homogeneous setup under SI voltage stresses. The value is in kV-peak.

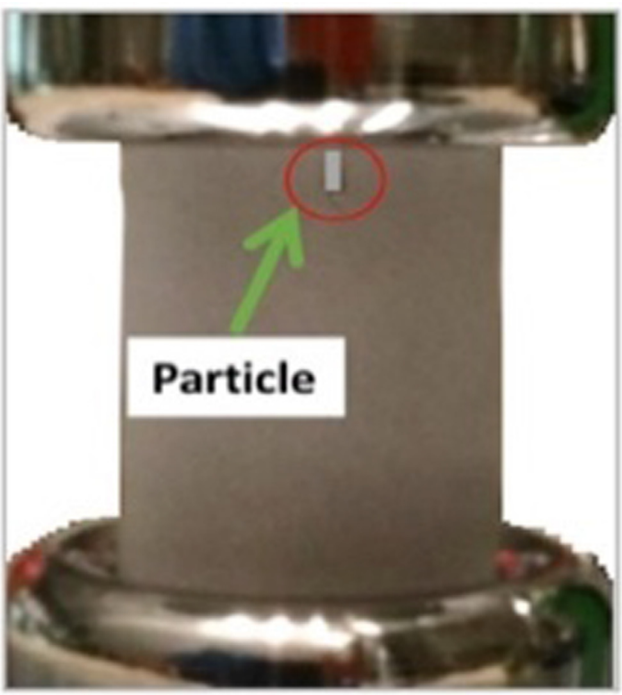

Fig. 16. The setup for inhomogeneous setup. A wire-like particle with a height of 2 mm (± 10%) and radius 0.25 (± 10%) mm was carefully attached on the surface epoxy sample close to the maximum curvature of a homogeneous configuration.

result from the test with 6000 ppmV was unclear and probably deviate with the expectation. The reason is probably, the corona stabilization was occurring at 6000 ppmV [12], but it is arguable and more samples are needed to obtain a firm conclusion.

6. Analysis: The influence of humidity on the flashover voltage

An analysis using best-fitting regression is used to estimate the mean value of the flashover voltage as a function of the gas pressure at a particular humidity content. The factor R^2 defines the curve fitness, where a value close to 1 means a good fit. Afterward, the ratio of the flashover voltage between humid and dry, or between higher and lower humidity content, is calculated. Table 4 provides the regression functions from all tests which are valid only within the gas pressures in the tests, whilst Table 5 provides the flashover voltage ratio from all tests.

As seen in Table 5, in general, at 3 and 4 bars gas pressures, in comparison to the dry condition, the addition of humidity slightly decreases the flashover voltage, but there is no consistent tendency that

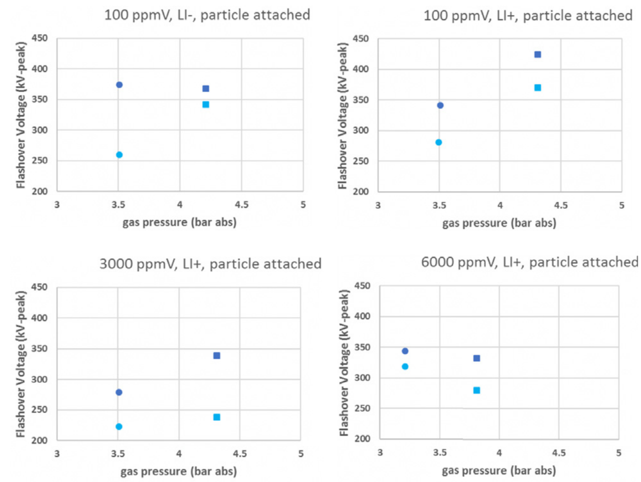

Fig. 17. The flashover voltage as a function of gas pressure at various humidity contents in the experiment with a particle attached to the epoxy sample, under LI+ and LI−. The value is in kV-peak.

Table 4

. Regression functions of the flashover voltage as a function of gas pressure at various humidity contents from all tests.

ppmV	Best Fit Regression	R^2 (%)	Regression Function (kV: Flashover Voltage, p: pressure in bar-abs)
Configuration: AC, Quasi homogeneous			
1000	Power	99.4	$kV = 86.112\ p^{0.7339}$
2000	Power	96.5	$kV = 79.096\ p^{0.772}$
4000	Power	99.3	$kV = 88.255\ p^{0.5941}$
6000	Linear	99.2	$kV = 30.65\ p + 71.348$
Sat.	Power	99.1	$kV = 85.776\ p^{0.6295}$
Cond.	–	–	–
Configuration: LI+, Quasi homogeneous			
1000	Power	98.5	$kV = 172.57\ p^{0.5872}$
4000	Power	98.4	$kV = 159.07\ p^{0.6324}$
6000	Power	98.1	$kV = 161.5\ p^{0.622}$
Sat.	Power	98.7	$kV = 168.07\ p^{0.5686}$
Cond.	–	–	–
Configuration: LI+, Homogeneous			
100	Exponential	90	$kV = 139.39\ e^{0.3855p}$
2000	Exponential	97.6	$kV = 172.5\ e^{0.3066p}$
Configuration: LI+, Particle Attached			
100	Linear	100	$kV = 109.38p - 71.312$
3000	Linear	100	$kV = 76p - 13.5$
Configuration: LI−, Quasi homogeneous			
1000	Polynomial	99.3	$kV = 6.1681\ p^2 + 56.977\ p + 104.17$
Saturation	Polynomial	99.9	$kV = 0.485\ p^2 + 72.954\ p + 104.38$
Configuration: SI, Quasi homogeneous			
1000	Polynomial	99.4	$kV = -3.6387\ p^2 + 89.702\ p + 66.442$
3000	Power	98.8	$kV = 116.54\ p^{0.762}$
4000	Polynomial	98.6	$kV = 0.6081\ p^2 + 73.157\ p + 51.087$
6000	Polynomial	100	$kV = -0.7357\ p^2 + 55.953\ p + 160.57$
Configuration: SI, Homogeneous			
100	Power	99.5	$kV = 145.04\ p^{0.742}$
2000	Linear	98.4	$kV = 78.182\ p + 90.746$
4000	Linear	100	$kV = 371.1\ \ln(p) - 139.74$
Saturation	Logarithmic	97.2	$kV = 89.189\ p + 31.703$

the higher humidity will decrease the flashover voltage. Only a small fraction of the result shows the higher flashover voltage at the higher humidity content.

In the test with the quasi-homogeneous setup under SI, the FO-ratio is peculiarly increasing as the humidity raised from 3000 to 6000 ppmV, at 3 and 4 bars.

The flashover voltage dropped by 21% when the humidity increases from 100 to 3000 ppmV, in the test with a particle attached on the

Table 5
The Flashover Voltage Ratio from all tests.

Gas Pressure (bars)	Humidity Content to compare (in ppmV) LOW	HIGH	Flashover (FO) Ratio (in %) = $FO_{at\ HIGH}/FO_{at\ LOW}$
Configuration: AC, Quasi homogeneous			
3	1000	2000	96%
	1000	4000	88%
	1000	6000	84%
	1000	Saturation	89%
2.6	1000	Condensation	≤72%
2	1000	Condensation	≤86%
Configuration: LI+, Quasi homogeneous			
3	1000	4000	97%
	1000	6000	97%
	1000	Saturation	95%
2.5	1000	Condensation	≤62%
Configuration: LI+, Homogeneous			
3	100	2000	**102%**
3.4	100	Condensation	≤33%
Configuration: LI+, Particle Attached			
4	100	3000	79%
Configuration: LI−, Quasi homogeneous			
4	1000	Saturation	94%
Configuration: SI, Quasi homogeneous			
3	1000	3000	89%
	1000	4000	91%
	1000	6000	**106%**
4	1000	3000	91%
	1000	4000	96%
	1000	6000	**102%**
Configuration: SI, Homogeneous			
4	100	2000	99%
	100	4000	96%
	100	Saturation	92%
	2000	4000	96%
	4000	Saturation	96%

epoxy. The inhomogeneity at the tip of the particle probably has more influence on the reduction of the flashover voltage, rather than due to the addition of humidity.

The flashover voltage in a homogeneous setup with and without a particle is compared under LI + at a gas pressure of 3.3 bars and humidity content of 100 ppmV. As a result, the presence of an attached particle in the setup has decreased the flashover voltage by 42%. This value is still below the reduction due to the condensation, which was 67% in a similar setup.

However, the calculation in this section is based on the mean flashover voltage, where a standard deviation above 10% has been found in the test. The deviation due to the addition of humidity content is still within the standard deviation, except when the condensation occurs, or when a particle is attached to the epoxy sample.

6.1. *A further analysis*

Further analysis from the other test under AC [2] has concluded that three parameters are influencing the flashover voltage, namely, the surface's condition of the epoxy, the gas pressure, and the humidity. The humidity (in vapor form) is the least significant parameter followed by the gas pressure. A decrease of 1 bar gas pressure could decrease the flashover by 28%.

The condition of the epoxy surface is the most significant parameter in the flashover voltage of the spacer. This finding has been proven by a series of tests under AC [2], with 3500 and 5000 ppmV. A decrease of flashover voltage by 50% had been observed after more than 100 times of flashovers. Following the test, significant depositions of white powder inside the test chamber, as well as carbonized tracks with

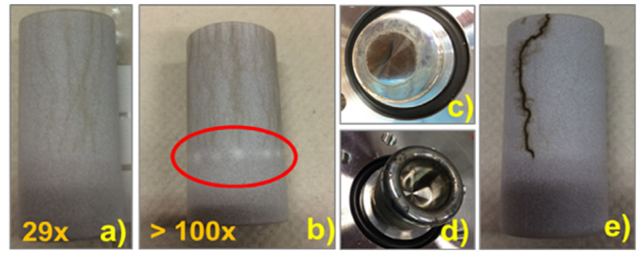

Fig. 18. (a) An epoxy sample after 29 flashovers. (b) Punctured points found close to the high electric field region after hundreds of flashovers. (c and d), the electrodes covered with decomposition by-products. (e) a carbonized track on the sample when the test was conducted without high-speed tripping circuit.

several punctured points close the high electric field region have been observed (see Fig. 18-b, 18-c, 18-d). The surface's condition includes the roughness of the surface and impurities deposited on the surface of solid insulation, particularly solid by-products and water droplets [13,14]. The presence of impurities with high dielectric constant, such as water (with a dielectric constant of 80), is responsible for the field enhancement on the surface of the epoxy sample that reduces the withstand strength of the gas-solid interface.

7. Conclusion

Humid SF_6 has been found in many non-CB enclosures in the case study of 631 bays of GIS installed on Java. The humidity mostly comes from the absorbed and adsorbed moisture at the internal parts of GIS, mainly in the spacer. The amount of moisture in GIS depends on the GIS design and the GIS handling.

The humidity did not influence the flashover voltage of the spacer as long there was no condensation. On the other hand, the gas pressure and the condition of the epoxy surface play significant roles in the flashover voltage. The findings agree with [13], and the results for only humid SF_6 are confirmed by [5].

Although the influence of humidity on the flashover voltage is neglectable, it becomes an agent in the creation of solid by-products that in the long run could significantly reduce the withstand strength of the insulation system, when discharges occur.

In the tests, the flashover reduction due to condensation was more prominent than due to an attached particle on the cast epoxy-resin sample.

Declaration of Competing Interest

The authors declared that there is no conflict of interest.

Acknowledgement

We dedicate this work to our beloved ones from the PLN TJBB who had passed away, Mrs. Ninil Ukhita Anggra Wardani, Mr. Ari Muchtar, and Mr. Denny Soeparjana, who had provided insights accordingly to their experiences in Asset Management and maintenance of GIS. This research has been technically and financially funded by PT. PLN (Persero), Indonesia.

References

[1] CIGRE WG A3.06, TB 513: Final Report of the 2004-2007, International Enquiry on Reliability of High Voltage Equipment, Part 5: Gas Insulated Switchgear (GIS), October 2012.
[2] Purnomoadi AP, Rodrigo Mor A, Smit JJ. Insulation Performance of GIS Operating Under Tropical Conditions. 20th ISH, Argentina; 2017.
[3] IEEE C37.122.5, IEEE Guide for Moisture Measurement and Control in SF6 Gas-Insulated Equipment; 2013.
[4] IEC 62271-1 Ed.1.0, High-voltage switchgear and controlgear – Part 1: Common specifications; 2007.

[5] Pharmatrisanti A. Long Term Performance of Gas Insulated Switchgear Operating Under Tropical Conditions. PhD Thesis, TU Delft, the Netherlands, June 2012.
[6] Chu FY, et al. A new approach to moisture measurement and control in Gas Insulated Switchgear. Proceedings of the Canadian Electrical Association, Engineering & Operating Division Meeting, Spring. 1986.
[7] Branscomb LM, Smith SJ. Electron affinity of atomic oxygen. Phys Rev 1955;98(4).
[8] Malik NH, et al. Electrical insulation in power systems. USA: Taylor and Francis Group; 1998.
[9] Naidu MS. Gas insulated substations. India, I.K: International Publishing; 2008.
[10] CIGRE WG B3.40, TB 723, SF6 Measurement Guide; 2018.
[11] IEC 60060-1, High-Voltage Test Techniques – Part 1: General definitions and test requirements, Edition-3; 2010.
[12] Purnomoadi AP. The influence of free moving particles on the breakdown voltage of GIS under different electrical stresses. Master Thesis, TU Delft, the Netherlands, 2012.
[13] Nitta T, et al. Factors controlling surface flashover in SF6 gas insulated systems. IEEE Trans Power Apparat Syst 1978.
[14] Laghari JR, Qureshi AH. Surface flashover of spacers in compressed gas insulated systems. IEEE Trans Electr Insul 1981.

Andreas Putro Purnomoadi is a High Voltage engineer from Perusahaan Listrik Negara (PLN), a state-owned electricity company in Indonesia. He studied electrical engineering and received a bachelor's degree from the Bandung Institute of Technology (ITB) in 2004 and an MSc degree from the Delft University of Technology in 2012. He is a PhD-Guest candidate at Department of DCE and S of TU Deflt, the Netherlands since October 2013. His research interests include health index model, condition assessment of high voltage apparatus, with now focusing on Gas Insulated Switchgear (GIS) operating under the tropical conditions.

Armando Rodrigo Mor is an Industrial Engineer from Universitat Politècnica de València, in Valencia, Spain, with a Ph.D. degree from this university in electrical engineering. During many years he has been working at the High Voltage Laboratory and Plasma Arc Laboratory of the Instituto de Tecnología Eléctrica in Valencia, Spain. Since 2013 he is an Assistant Professor in the Electrical Sustainable Energy Department at Delft University of Technology, in Delft, the Netherlands. His research interests include monitoring and diagnostic, sensors for high voltage applications, high voltage engineering, and HVDC.

Johan J. Smit is professor at the Delft University of Technology (The Netherlands) in High Voltage Technology and Management since 1996 and emeritus since 2015. After his graduation in experimental physics he received his PhD degree from Leiden University in 1979. After his research in cryogenic electromagnetism at the Kamerlingh Onnes Laboratory, he was employed as T&D research manager at KEMA's laboratories in Arnhem-NL for 20 years. Furthermore, he was director of education in electrical engineering, supervisory board member of the power transmission company of South Holland, and CEO of the asset management foundation Ksandr for 10 years. In 2003 he was general chairman of the International Symposium on HV Engineering in Delft. He is TC-honorary member of CIGRE and past chairman of CIGRE D1 on Materials & Emerging Technologies. Currently he is convener of the area Substation Management for CIGRE B3 and he holds the international chair of Technical Committee IEC112 on Electrical Insulation Systems.